

MBMA ⁹⁰⁰⁶
506

Loc: S 3

FINAL REPORT

X-BRACING ANCHORAGE CONNECTION UNDER STATIC AND SEISMIC LOADING CONDITIONS

eirs

ENGINEERING & INDUSTRIAL RESEARCH STATION

By

**R. Ralph Sinno, Ph.D., P.E.
Professor
Department of Civil Engineering**

**Engineering and Industrial Research Station
Mississippi State University
Mississippi State, MS 39762**

January 1992

MSSU-EIRS-CE-91-1

COLLEGE OF ENGINEERING ADMINISTRATION

ROBERT A. ALTENKIRCH, PH.D.
DEAN, COLLEGE OF ENGINEERING

WALTER R. CARNES, PH.D.
ASSOCIATE DEAN

JOHN I. PAULK, PH.D.
ASSOCIATE DEAN

LAWRENCE J. HILL, M.S.
DIRECTOR, ENGINEERING SERVICES

CHARLES B. CLIETT, M.S.
AEROSPACE ENGINEERING

WILLIAM R. FOX, PH.D.
AGRICULTURAL & BIOLOGICAL ENGINEERING

DONALD O. HILL, PH.D.
CHEMICAL ENGINEERING

JOSEPH H. SHERRARD, PH.D.
CIVIL ENGINEERING

B. J. BALL, PH.D.
ELECTRICAL ENGINEERING

LARRY G. BROWN, PH.D.
INDUSTRIAL ENGINEERING

C. T. CARLEY, PH.D.
MECHANICAL & NUCLEAR ENGINEERING

RUDY E. ROGERS, PH.D.
PETROLEUM ENGINEERING

For additional copies or information
address correspondence to:

ENGINEERING AND INDUSTRIAL RESEARCH
STATION
DRAWER DE
MISSISSIPPI STATE UNIVERSITY
MISSISSIPPI STATE, MISSISSIPPI 39762

TELEPHONE (601) 325-2269



Mississippi State University does not discriminate on the basis of race, color, religion, national origin, sex, age, or against handicapped individuals and Vietnam—era veterans.

In conformity with Title IX of the Education Amendments of 1972 and Section 504 of the Rehabilitation Act of 1973, Joyce B. Giglioni, Assistant to the President, 610 Allen Hall, P. O. Drawer J, Mississippi State, Mississippi 39762, office telephone number 325-2231, has been designated as the responsible employee to coordinate efforts to carry out responsibilities and make investigation of complaints relating to discrimination.



FINAL REPORT

X-BRACING ANCHORAGE CONNECTION UNDER STATIC AND SEISMIC LOADING CONDITIONS

By

**R. Ralph Sinno, Ph.D., P.E.
Professor
Department of Civil Engineering**

**Engineering and Industrial Research Station
Mississippi State University
Mississippi State, MS 39762**

January 1992

MSSU-EIRS-CE-91-1

PREFACE AND ACKNOWLEDGEMENTS

The study reported herein was sponsored by the Metal Building Manufacturers Association (MBMA), Cleveland, Ohio. Test specimens were supplied by Butler Research, Ceco Building Division, and Gulf States Manufacturers. The research work was conducted in consultation with the Primary Framing Subcommittee and the Director of Research and Engineering of MBMA.

The opinions, findings, and conclusions expressed herein are those of the writer and are not necessarily those of the MBMA.

X-BRACING ANCHORAGE CONNECTION UNDER STATIC AND SEISMIC LOADING CONDITIONS

ABSTRACT: Current practice of anchoring x-bracing rods in low-rise metal buildings uses the web of the steel framing for a positive stop. The tension-only bracing rod rests on a hillside washer. Thus, the anchorage connection is subjected to a high concentration of a direct punching load raising the question about the adequate strength needed for the normally thin web to resist the direct pull-out force. The ultimate strength of such a connection is not documented in the literature from either analytical or experimental viewpoint and it is not covered in the common design standards.

A comprehensive experimental laboratory testing program was designed to investigate the major parameters influencing the ultimate load carrying capacity of the anchorage connection detail. A finite element program based on elastic analysis was used to establish significant information on the level and distribution of the stresses around the anchorage connection, and to isolate the interdependencies of the multiple variables involved. Thirty-five direct pull-out laboratory tests were performed using static and repetitive tensile cyclic loading. The parameters in these tests covered four rod sizes and corresponding hillside washers, three web thicknesses, and two methods for stiffening the web plate; namely by using a patch plate around the anchorage slotted hole and by placing horizontal stiffener plates.

The finite element elastic analysis approach was known to be inadequate to predict the ultimate load capacity, and for this reason a yield line approach, limit state analysis, was used to perform the prediction process. Five failure mechanisms were isolated and identified. The results from the analytical expressions derived for each of the failure mechanisms were compared to those from the experimental testing program. The yield line limit state design approach was found to predict very well the failure mode and the ultimate load carrying capacity of the x-bracing rod anchorage connection. Repetitive tensile loading conditions simulating seismic loading up to the yield point of the x-bracing rod did not cause serious deterioration to the strength of the connection after 20 cycles of tensile loading.

TABLE OF CONTENTS

	<u>Page</u>
PREFACE AND ACKNOWLEDGEMENTS	ii
ABSTRACT	iii
INTRODUCTION	1
LITERATURE REVIEW	2
OBJECTIVES	5
EXPERIMENTAL INVESTIGATION	6
TEST RESULTS	10
Series CC	15
Series GP	17
Series BS	18
ELASTIC ANALYSIS - FINITE ELEMENT APPROACH	20
ANALYTICAL INVESTIGATION	24
FAILURE MECHANISMS AND ANALYTICAL CALCULATIONS	27
- Failure Mechanism 1	27
- Failure Mechanism 2	28
- Failure Mechanism 3	30
- Failure Mechanism 4	31
- Failure Mechanism 5	32
COMPARISON OF EXPERIMENTAL VERSUS ANALYTICAL RESULTS	33
REPETITIVE TENSILE LOADING TESTS - SEISMIC LOADING	35
CONCLUSIONS	47
APPENDIX I. REFERENCES	49
APPEXDIX II. NOTATION	50
APPENDIX III. DESIGN OF ANCHORAGE CONNECTION USING <u>ALLOWABLE STRESS DESIGN (ASD)</u>	51
APPENDIX IV. NUMERICAL EXAMPLE	53
APPENDIX V. CONVERSION TO SI UNITS	54

X-BRACING ANCHORAGE CONNECTION UNDER STATIC AND SEISMIC LOADING CONDITIONS

INTRODUCTION

Current practice of anchoring x-bracing rods in low-rise metal buildings uses the web of the I-section of the structural framing for a positive stop. A slotted hole is punched into the web, and the threaded x-bracing rod is inserted through the hole to be locked in place by a threaded nut bearing against a hillside washer. The flat bearing surface of the hillside washer bears on the thin web and is locked in place by a protruding nipple that fits into the rounded upper edge of the slotted hole. Hence, the tensile x-bracing rod causes direct punch-bearing pressure of the flat base and nipple of the hillside washer against the thin web of the framing section. The vertical angle that the x-bracing rod makes with the web of the section varies with the rise to bay spacing ratio of the structural framing. This angle has a direct influence on the distribution of stresses and the overall strength of the connection.

Certain metal building manufacturers select to use high strength steel cables for the x-bracing instead of solid rods. This practice has no significant impact on the objectives and findings of this report provided that the anchorage connection details are similar to those described here.

The web plates of the metal framing section supporting the anchorage of the x-bracing rods are usually quite thin with the unsupported depth to thickness ratio of 100-200. This causes the anchorage mechanism to behave in a very flexible manner. Also, the

thin web raises the potential of the hillside washer to pull out through the slotted hole, either by direct shear punching or by tensile tearing of the bearing contact area. Furthermore, the fillet welds between the thin web and the flanges of the framing I-section are subjected to high concentrations of stresses that are not usually considered in the structural design and proportioning of the section of the framing system.

In the present design procedures, the x-brace is intended to resist the lateral forces from the wind loads. Under seismic loading conditions of moderate to high intensity, the design lateral forces carried by the bracing rods could reach high levels of concentration. Furthermore, these dynamic lateral forces could be coupled with a serious potential for impact factors due to the extreme slenderness of the rods. It is recommended by SEAOC (1990) that the bracing members resist most of the lateral forces in a major earthquake, and the design forces need to develop at most the tensile yield strength of the bracing rod. These same minimum strength requirements for the brace must also apply to the design of the anchorage connections as they are a part of the bracing system.

The lateral tensile force in a bracing member in a major earthquake is expected to exceed the force caused by high wind forces. The requirement in current design recommendations for magnified and factored effects associated with any seismic analysis made it necessary to investigate in detail the currently used x-bracing anchorage system. The testing program reported here attempts to encompass the analytical procedure for evaluating the

load transfer mechanism of the anchorage connection under static and repetitive loading conditions up to the collapse point, while keeping in mind the desirability to avoid any brittle failure of the brace connection itself.

LITERATURE REVIEW

X-bracing rods or cables have been in use to resist lateral forces in low-rise metal buildings for a long time. The dependency on this tensile tie bracing system is based on assuming buckled configuration on the other side of the x-brace. The system has performed well over the years. Failures associated with the tie bracing in resisting wind lateral loading have been isolated and are rather rare. Documented earthquake failures attributed to the tie rod x-bracing systems are non-existent in the literature. In a recent building survey of the Epicenter Area after the Loma Prieta (San Francisco) Earthquake of October 17, 1989, (MBMA 1990), the x-bracing connections and rods sustained no recorded damage in any of the inspected metal building frames in the area. However, in reviewing the literature it is found that certain design limitations on structural framing utilizing the contribution of x-bracing to resist seismic lateral forces are well covered by many researchers and publications (SEAOC 1990; Hwang et. al. 1989, Popov and Black, 1981; Chang et. al. 1989; MBMA 1986).

The ultimate load carrying capacity of the x-bracing anchorage connection as used in current practice is normally based on empirical relationships supported by limited proprietary tests and the experience of the individual manufacturer. The strength and

behavior under load of the connection and the contribution of stiffeners to the thin web, when stiffeners are used to support these connections, are not known. Experimental test results supporting or forming the reference for a comprehensive design approach are not found in the literature.

The analysis of stresses in thin webs with holes has received the analytical and experimental attention of several researchers. The major concern in these studies has been the overall strength of the structural members in carrying the design loads. Similarly, the stress analysis of thin webs supported by stiffener plates placed transversely and laterally has considerable coverage in the literature. But, the theoretical and experimental evaluation of the strength of the anchorage connection itself, with and without stiffeners, in carrying the x-bracing tensile force has not been studied. This report addresses this problem through experimental testing and analytical formulations for the prediction of the ultimate load carrying capacity of the anchorage connection.

In keeping with the nature of the problem, a limit state design philosophy is recommended to be used. This approach fits with the current trend toward load and resistance factor method (LRFD) for structural steel design (AISC, 1986). It is imperative to note that the presence of severe local stress concentrations, residual stresses, and combined stresses in all forms at the connection makes the use of an elastic or an elasto-plastic strength analysis inadequate to predict the ultimate load carrying capacity and the associated failure mode.

OBJECTIVES

The need for a comprehensive analytical approach for determining the behavior and ultimate capacity of the x-bracing anchorage connection in low-rise metal buildings under static and seismic loading conditions necessitated this research project. A comprehensive experimental testing program was executed to observe the potential failure mechanisms and the influence of the inherent variables on the ultimate load carrying capacity of the connection.

The present design procedure for selecting the x-bracing is concentrated on estimating the magnitude of the lateral wind forces followed by an approximate design formulations for the sizing and proportioning of the connection detail. The primary objective of this research work was to establish performance criteria of the connection under load and to develop analytical formulations for predicting its ultimate load carrying capacity.

It has been established that lateral wind forces carried by x-bracing tensile rods are relatively easier to predict than those caused by the dynamic seismic forces. In the design for earthquakes by almost all of the applicable seismic design criteria, usually certain magnification factors have been required or recommended to be included in the design of the x-bracing rod and anchorage connections (SEAOC 1990; MBMA 1986). The secondary objective of this research was to evaluate, on the basis of laboratory test results, the performance of the anchorage connection under simulated seismic loading conditions.

The experimental laboratory testing program was divided into two main sets of tests. The first set covered the static testing

of the connection. This set served the objective of isolating the different potential failure mechanisms and related problem areas.

The second set carried the findings one step further by focusing on the deterioration of the strength of the connection under high rate of repetitive loading of tensile forces. The significance of impact loading usually associated with seismic loading conditions and that might jeopardize the ultimate load carrying capacity of the connection was also observed.

EXPERIMENTAL INVESTIGATION

Static and repetitively loaded direct pull-out tests were performed to evaluate the ultimate load carrying capacity of the anchorage connection of the x-bracing. The parameters were isolated and were explored in a sequential order to eliminate, where possible, certain controlling mechanisms of failure. This approach was assisted by the findings from a computer program using elastic analysis.

Certain parameters were kept unchanged in all of the tests. These were the size and location of the web-flange fillet weld, the location of the anchorage point of the rod, and the angle between the rod and the web of the section. Only the most commonly used range for the parameters were tested. The test set-up used in performing the pull-out tests is shown in Fig. 1. The location of the tensile force of the x-brace was kept at a distance of 2.5 in. from the adjacent flange, and 14 in. from the second flange as shown in Fig. 2.

The variable parameters in the experimental laboratory tests

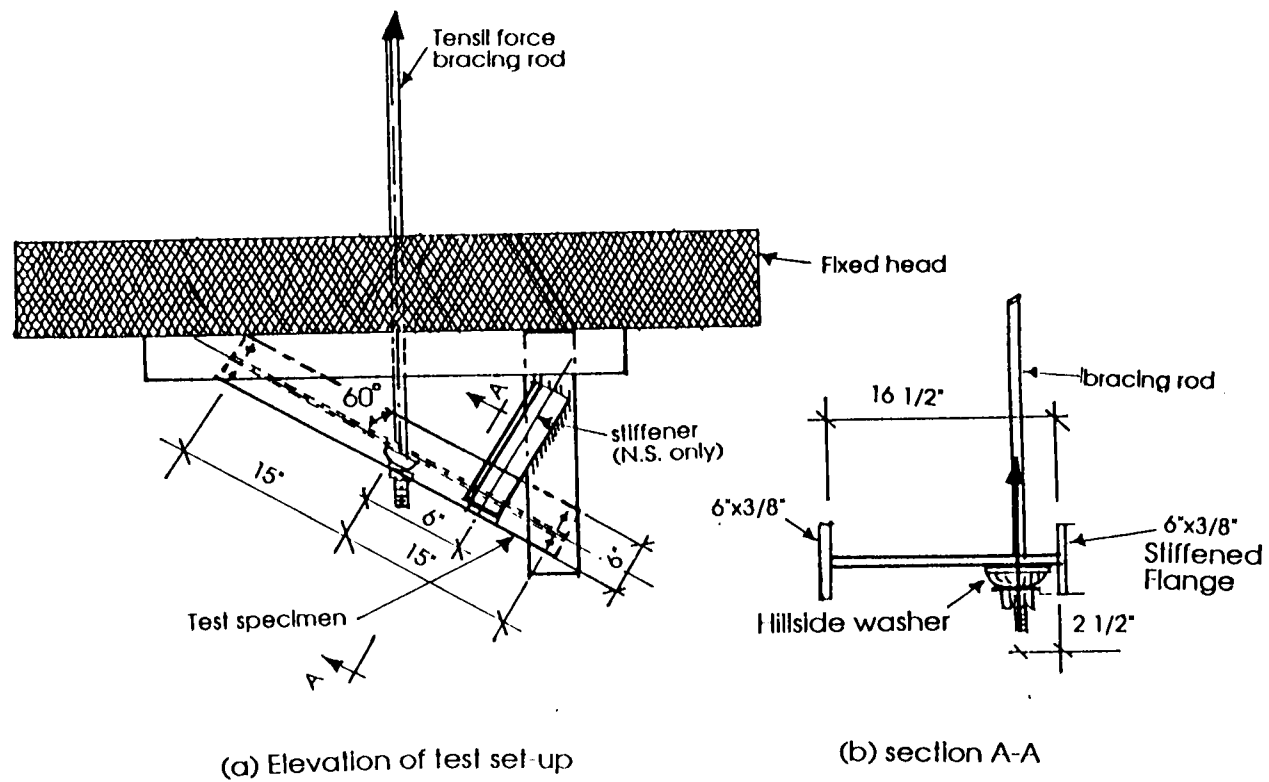


FIG. 1. Set-up for Performing the Pull-out Tests

were the following:

1. The diameter of the x-bracing rod and the corresponding size of the anchorage hillside washer.
2. The thickness of the web of the structural framing section.
3. Stiffening of the web plate by adding a $5 \frac{3}{4} \times 3 \frac{7}{8} \times \frac{1}{4}$ in. reinforcing patch plate welded all around to the web of the section - Series GP.
4. Stiffening of the web plate by using two $16 \frac{1}{2} \times \frac{1}{4}$ in. transverse stiffener plates placed 6 in. from the slotted hole of the x-bracing rod - Series BS.

The size of the weld between the web of the framing section and the flanges was not intended to be a variable parameter in the planning of the test specimens (Fig. 2), but was noted to vary during testing the individual specimens. The original details of the test specimens called for $\frac{3}{32}$ in. weld on one side of the web. However, the actual test specimens were supplied by different metal building manufacturers and did not have a constant size weld. Accordingly, the weld size next to the anchorage slotted hole for the x-brace was visually inspected, measured, and rated at the time each test was performed. The average size was used in the analytical calculations for each test. Also, the weld penetration was not always uniform along the length of the web-flange connection, and certain test specimens were over welded and carried two passes of weld line. These observations caused certain inconsistencies in the results of tests that were supposed to be similar.

Static tests up to the failure loads were performed on 25 test specimens followed by repetitive loading tests on 10 selected test specimens. On the basis of the results observed from the static tests, the magnitudes of the repetitive cyclic loads were set so that yielding of some part of the anchorage connection took place. The repetitive loads were cycled between a predetermined maximum load and a minimum of 500 lbs. tensile load for 20 cycles. If no failure occurred during the repetitive cycle loading, then the tensile loading continued until failure.

TEST RESULTS

The yield and ultimate strength of the x-bracing rods, with failure at the threaded section, were determined in separate direct tension tests. The yield and ultimate strength of the steel plates used in making the webs of the structural framing sections were also determined from tension coupons cut from the web plates of the sections.

The test results from the direct tension tests on the rods and the web plates are shown in Tables 1 and 2, respectively.

The test specimens were supported at both ends in a testing frame as shown in Fig. 1. An additional support was used to hold one flange of the section in place at 6 in. from the x-bracing anchorage connection. This added support was used to simulate the tie usually provided by the girts or purlins in the full-size structural framing.

Table 1. Direct Tension Tests on Web Plates

Series (1)	Yield Strength (psi) (2)	Ultimate Strength (psi) (3)	Effective Yield Strength (psi) (4)
CC	61,100	83,000	75,700
	56,300	78,200	70,900
	60,857	82,160	75,059
Average	59,419	81,120	73,886
GP	59,800	74,700	69,733
	55,800	72,700	67,067
	56,700	73,800	68,100
Average	57,433	73,733	68,300
BS	58,170	85,500	76,390
	55,500	84,100	74,566
	55,800	84,800	75,133
Average	56,490	84,800	75,363

Table 2. Direct Tension Tests on Threaded Section of X-bracing Rods

Rod Dia. (in.) (1)	Yield Force (lbs.) (2)	Ultimate Force (lbs.) (3)	Effective Yield Force (lbs.) (4)
1/2 (Threaded area = 0.140 in ²)	10,400	10,820	10,680
	10,100	10,710	10,506
	10,200	10,840	10,627
	9,300	10,750	10,266
	9,500	11,080	10,553
	Average	10,840	10,527
5/8 (Threaded area = 0.220 in ²)	15,500	16,500	16,167
	15,550	16,000	15,850
	15,750	17,080	16,637
	15,850	16,870	16,530
	15,740	16,870	16,493
	15,500	17,100	16,567
	Average	16,736	16,374
3/4 (Threaded area = 0.363 in ²)	24,000	28,300	26,867
	24,000	28,800	27,200
	23,500	28,700	26,967
	25,750	29,250	28,083
	Average	28,762	27,278
1 (Threaded area = 0.628 in ²)	42,250	51,800	48,617
	42,250	52,200	48,883
	42,200	50,800	47,934
	Average	51,600	48,478

Table 3. Test Specimens Parameters - Static Tests

Test No.	Test Specimen*	PROPERTIES					
		Web (t_w) (in.)	Web Stiffener	Rod (d) (in.)	Washer Size (in.)	Web-Flange Weld	
						Leg Size (in.)	Rating
(1)	(2)	(3)	(4)	(5)	(6)	(7)	(8)
1	CC 1/8 R 1/2A*	0.126	_____	1/2	1/2	0.11	Fair
2	CC 1/8 R 1/2B	0.126	_____	1/2	5/8	0.15	Two Passes
3	CC 1/8 R 5/8A	0.129	_____	5/8	5/8	0.16	Two Passes
4	CC 1/8 R 5/8 B	0.126	_____	5/8	3/4	0.16	Two Passes
5	CC 1/8 R 3/4 A	0.127	_____	3/4	3/4	0.10	Uneven Weld
6	CC 1/8 R 3/4 B	0.129	_____	3/4	3/4	0.11	Fair
7	CC 1/8 R 3/4 C	0.127	_____	3/4	3/4	0.11	Fair
8	CC 3/16 R 5/8	0.183	_____	5/8	5/8	0.12	Fair
9	CC 3/16 R 3/4 A	0.186	_____	3/4	3/4	0.11	Fair
10	CC 3/16 R 3/4 B	0.186	_____	3/4	3/4	0.11	Fair
11	CC 3/16 R 3/4 C	0.183	_____	3/4	3/4	0.12	Good
12	CC 1/4 R 3/4	0.249	_____	3/4	3/4	0.17	Two Passes
13	CC 1/4 R 1 A	0.249	_____	1	1	0.12	Uneven Weld
14	CC 1/4 R 1 B	0.249	_____	1	1	0.17	Two Passes
15	GP 1/8 R 1/2	0.119	Patch Plate	1/2	1/2	0.20	Excellent
16	GP 1/8 R 3/4A	0.119	Patch Plate	3/4	3/4	0.20	Excellent
17	GP 1/8 R 3/4B	0.119	Patch Plate	3/4	3/4	0.20	Excellent
18	GP 3/16 R 1	0.178	Patch Plate	1	1	0.20	Excellent
19	BS 1/8 R 3/4A	0.118	Trans. Stiffeners	3/4	3/4	0.18	Good
20	BS 1/8 R 3/4B	0.118	Trans. Stiffeners	3/4	3/4	0.18	Good
21	BS 3/16 R 5/8	0.177	Trans. Stiffeners	5/8	3/4	Double Passes/Over Welding	
22	BS 3/16 R 3/4	0.177	Trans. Stiffeners	3/4	3/4	0.19	Good
23	BS 3/16 R 1	0.177	Trans. Stiffeners	1	1	Double Passes/Over Welding	
24	BS 1/4 R 1A	0.249	Trans. Stiffeners	1	1	0.19	Good
25	BS 1/4 R 1B	0.249	Trans. Stiffeners	1	1	Double Passes/Over Welding	

* Test specimen designation: CC = Series; 1/8 = web thickness; R1/2 = X-bracing rod diameter; A = Test A.

Table 4. Comparison of Experimental and Analytical Results-Static Tests

Test No.	Test Specimen	Ultimate Loads (lbs.)						Ratio: $\frac{P_{uexp}}{P_u}$	Failure Mode	
		Experiment P_{uexp}	Analytical as per Failure Modes						Test	Theory
			P_{u1}	P_{u2}	P_{u3}	P_{u4}	P_{u5}			
(1)	(2)	(3)	(4)	(5)	(6)	(7)	(8)	(9)	(10)	(11)
1	CC 1/8 R 1/2A	8,840	10,527	14,850	28,727	<u>7.791</u>	8,380	1.13	4	4
2	CC 1/8 R 1/2B	10,800	<u>10.527</u>	22,046	31,030	12,592	12,820	1.02	1	1
3	CC 1/8 R 5/8B	15,250	16,374	23,515	31,768	<u>12.892</u>	<u>13.102</u>	1.18	4	4 or 5
4	CC 1/8 R 5/8A	15,000	<u>16.374</u>	26,861	35,443	28,224	21,721	0.92	1	1
5	CC 1/8 R 3/4A	14,800	27,278	<u>16.788</u>	35,725	28,447	21,885	0.88	2	2
6	CC 1/8 R 3/4B	18,750	27,278	<u>18.467</u>	36,288	28,896	22,211	1.02	2	2
7	CC 1/8 R 3/4C	18,000	27,278	<u>18.467</u>	35,725	28,447	21,885	0.98	2	2
8	CC 3/16 R 5/8	17,000	<u>16.374</u>	17,637	45,066	18,289	18,020	1.04	1	1
9	CC 3/16 R 3/4A	17,500	27,278	<u>18.467</u>	52,321	41,663	31,308	0.95	2	2
10	CC 3/16 R 3/4B	17,750	27,278	<u>18.467</u>	52,321	41,663	31,308	0.96	2	2
11	CC 3/16 R 3/4 C	22,500	27,278	<u>20.145</u>	51,478	40,992	30,840	1.12	2	2
12	CC 1/4 R 3/4	28,300	<u>27.278</u>	28,540	70,044	55,775	40,898	1.04	1	1
13	CC 1/4 R 1A	25,000	48,478	<u>23.178</u>	80,586	82,890	57,292	1.08	2	2
14	CC 1/4 R 1B	32,350	48,478	<u>32.836</u>	80,586	82,890	57,292	0.99	2	2
15	GP 1/8 R 1/2	10,750	<u>10.527</u>	38,189	24,882	21,091	19,300	1.02	1	1
16	GP 1/8 R 3/4A	23,850*	<u>27.278</u>	47,491	30,944	76,406	53,559	—	—	—
17	GP 1/8 R 3/4B	24,000*	<u>27.278</u>	47,491	30,944	76,406	53,559	—	—	—
18	GP 3/16 R1	37,250*	<u>48.478</u>	54,640	53,253	141,445	86,400	—	—	—
19	BS 1/8 R 3/4A	17,950	27,278	30,218	33,857	23,997	<u>18.406</u>	0.98	5	5
20	BS 1/8 R 3/4B	18,200	27,278	30,218	33,857	23,997	<u>18.406</u>	0.99	5	5
21	BS 3/16 R 5/8	17,050	<u>16.374</u>	—	50,785	35,995	26,988	1.04	1	1
22	BS 3/16 R 3/4	28,700	<u>27.278</u>	31,897	50,785	35,996	<u>26.988</u>	1.03	1	1 or 5
23	BS 3/16 R 1	40,050	48,478	—	58,430	60,100	<u>38.904</u>	1.03	5	5
24	BS 1/4 R 1A	38,000	48,478	<u>36.698</u>	82,198	84,548	53,595	1.04	2	2
25	BS 1/4 R 1B	50,700	<u>48.478</u>	—	82,198	84,548	53,595	1.04	1	1

* Test terminated before connection failure is reached because of excessive deflection of web and deformation of entire test section.

The basic parameters of the test specimens are shown in Table 3. The test results are given in Table 4, and Col. 3 gives the experimental ultimate loads and Col. 10 gives the test failure modes. The following notation is used:

Mode 1: Tensile fracture of the x-bracing rod.

Mode 2: Failure of the fillet weld between the web plate and the flange of the section adjacent to the anchorage connection.

Mode 3: Direct shear fracture of the web plate at the edge of the adjacent web-flange fillet weld.

Mode 4: Punching shear fracture of the web plate beneath the hillside washer.

Mode 5: Tensile fracture of the anchorage slotted hole in the web plate of the section beneath the hillside washer.

TEST RESULTS OF SERIES CC: No web stiffeners were used in this series of tests.

Tests No. 1 and 2: These two tests were identical except for the size of the hillside washer. The 1/2 in. hillside washer in Test No. 1 punched through the web plate of the section at the ultimate load. In Test No. 2, the anchorage connection was capable of carrying the full strength of the 1/2 in. diameter x-bracing rod by using a 5/8 in. hillside washer. Thus, the failure mode in Test No. 2 was by tensile failure of the x-bracing rod.

Tests No. 3 and 4: These two tests were a repeat of Tests No. 1 and 2 except for the size of the hillside washers. The hillside

washer was 5/8 in. in Test No. 3 and 3/4 in. in Test No. 4. In the two tests, the observed failure modes confirmed that the size of the flat bearing base of the hillside washer influenced the ultimate load carrying capacity of the anchorage connection.

Tests No. 2 and 3: The two tests were identical except for the size of the x-bracing rods. The diameter of the rod was increased from 1/2 in. in Test No. 2 to 5/8 in. in Test No. 3. The rod failure that occurred in Test No. 2 was prevented in Test No. 3.

Tests No. 4 and 5, 6, 7: The tensile failure of the x-bracing rod of Test No. 4 was prevented by increasing the size of the rod from 5/8 in. to 3/4 in. in Tests No. 5, 6, and 7 while other parameters remained the same. The web-flange fillet weld failed in Tests Nos. 5, 6, and 7.

Tests No. 8 and 9, 10, 11: The x-bracing rod failed in Test No. 8 where a 5/8 in. hillside washer was used. This rod tensile failure was prevented in Tests No. 9, 10, and 11 where the size of the hillside washer and the rod were both increased from 5/8 in. to 3/4 in. and the failure occurred in the web-flange weld.

Tests No. 12 and 13, 14: In Test No. 12, the 3/4 in. diameter x-bracing rod failed in tension. When the rod was increased to 1 in. in diameter in Tests No. 13 and 14, and with a 1 in. hillside washer, the rod did not fail in tension. The web to flange fillet weld failed in the last two tests.

In summary, the static tests performed on Series CC were used to isolate and demonstrate the different failure mechanisms. The contribution of each of the variable parameters to the ultimate

load carrying capacity of the x-bracing was carefully evaluated and noted. It was possible to achieve the tensile yield strength of the bracing rod in all of the test set-ups. The area and the geometry of the flat bearing base of the hillside washer influenced significantly the ultimate load carrying capacity of the connection. The tests have also shown that an adequate size of web-flange weld is needed for a proper and balanced design. The required size of weld between the web and the flange might exceed that used in the built-up section of the framing. The tests demonstrated that the size of the slotted hole for anchoring the x-bracing rod and the size of the flat base of the hillside washer need to be coordinated. For thin webs, and with large size slotted holes, the punching fracture of the web plate under the hillside washer was critical. Failure of the web plate in flexure was not a serious problem as it did not dominate the failure mode in any of the tests.

TEST RESULTS OF SERIES GP: In this series of tests, a flat patch plate was used as a stiffener to the web plate of the section. The patch plate was $5 \frac{3}{4} \times 3 \frac{7}{8} \times \frac{1}{4}$ in. welded all around the web plate using $\frac{1}{4}$ in. fillet weld. An automatic submerged arc welding (SAW) was used for the web-flange weld line in this series. The weld was uniformly placed with full penetration.

Test No. 15: This test was a repeat of test No. 1 where the hillside washer punched through the thin web of the section. In this test, the rod failed in tension.

Tests No. 16, 17 18: The patch plate in these tests provided more

than adequate strength to the anchorage bearing area. The loading was terminated at the load shown in Table 4, Col. 3, before failure occurred due to excessive deformation of the web plate and the entire test section.

This series of tests confirmed that failure of the anchorage connection was a localized phenomena concentrated around the hillside washer. The size of the hillside washer defined the extent of the highly stressed areas. -

TEST RESULTS OF SERIES BS: In this series of tests, two transverse stiffener plates 16 1/2 x 3/4 in. were placed on both sides of the web at 6 in. from the slotted hole. The use of these two stiffener plates was considered in the testing program for two reasons: (a) To stiffen the web plate in a simulation of the stiffeners normally used at rafter ends and knee joints of the framing system, and (b) to simulate the base plate at the bottom of the column of the structural framing.

Tests No. 19 and 20: The set-ups for these two tests were identical, and the test results were similar. The failure mode was localized to the web plate beneath the flat contact area of the hillside washer. Tension fracture of the two longitudinal sides of the slotted hole took place. These two tests were also a repeat of test Nos. 5, 6, and 7 of Series CC, with the exception of the size of the slotted hole and the size of the web-flange weld. The improved weld in this series shifted the failure mechanism to the anchorage connection itself where the larger 2 x 1 in. slotted hole caused the thin web plate to fracture under the tensile component

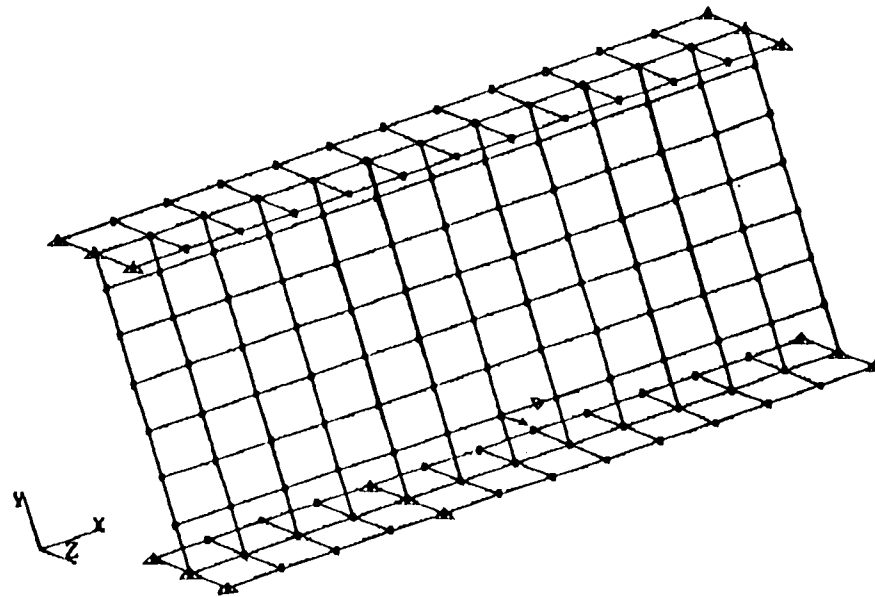


FIG. 3. Finite Element Grid for Elastic Analysis

of the pressure of the concentrated punching load.

Tests No. 21 and 22: These two tests were a repeat of tests No. 8 and 9, 10, 11, respectively, of Series CC. The failure modes confirmed the weakness of the localized area under the hillside washer. The contribution of the transverse stiffener plates to the load carrying capacity of the anchorage connection was minimal.

The load-deflection shape of the specimens with transverse stiffener plates welded to the web showed considerable restraint-as the loading progressed beyond yielding of the web plate. However, this added stiffness to the section did not strengthen or prevent the local failure of the web plate around the hillside washer.

The failure modes and the prediction of the failure loads were investigated using the observations noted during the actual performance of the tests and from the experimental test results. The analytical formulations for the calculations of the ultimate load carrying capacity for each of the failure modes are discussed in the following sections.

ELASTIC ANALYSIS - FINITE ELEMENT APPROACH

Elastic analysis using finite element approach was used to gain a significant feel for the level and the distribution of the stresses around the x-bracing anchorage connection. The grid for the finite elements and the support conditions to the framing test section that were used in the computer analysis are shown in Fig. 3. The elastic analysis approach was performed although it was inadequate to predict the ultimate load capacity and the failure

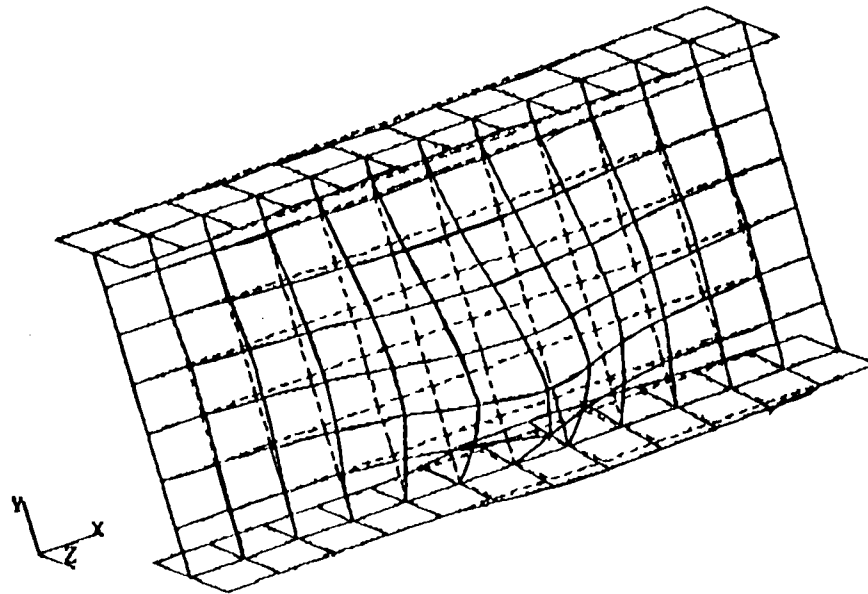


FIG. 4. Typical Deflected Shape by Elastic Analysis

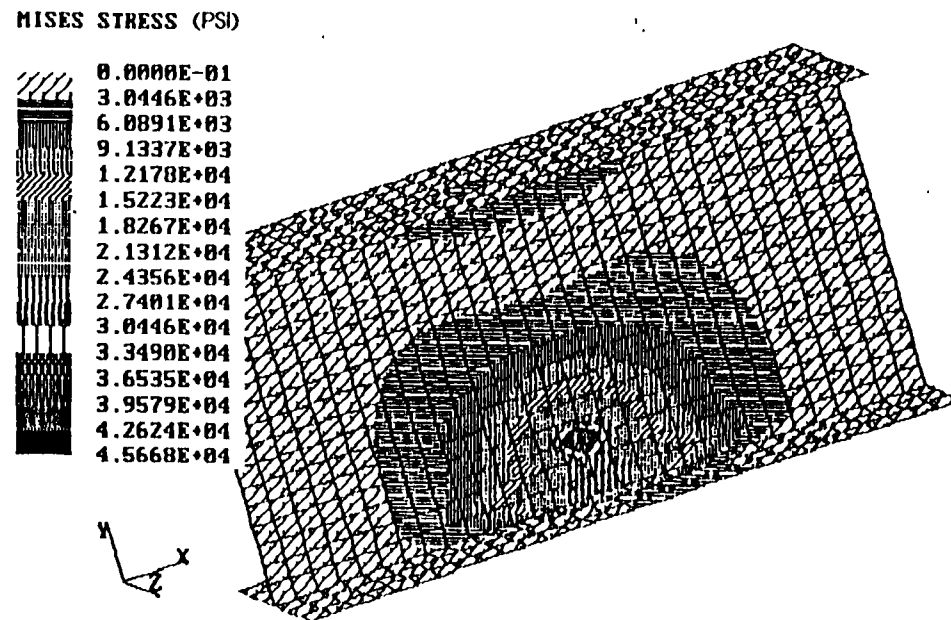


FIG. 5. Stress Contours by Elastic Analysis

modes of the anchorage connection. The finite element analysis did not allow for the stress concentrations, the residual stresses, and the redistribution of stresses in the connection. It was used strictly to ascertain that the size of the test specimen was adequate to encompass the distribution of the generated stresses and to isolate the impact of each of the variable parameters on the stress distribution around the anchorage connection. The results from the elastic analysis proved helpful in providing the analytical data on the elastic deflected shape of the test specimens caused by the oblique concentrated pull-out force. The distribution of the combined stresses in the connection when carried beyond the elastic zone were found to be highly indeterminate and could not be analyzed without extensive assumptions.

The number of test specimens required to be tested to satisfy the objectives of this study were reduced considerably as a result of the knowledge provided by the computerized elastic analysis. The results of a typical finite element elastic analysis are shown in Figs. 4, and 5.

The following general comments can be made on the basis of the answers provided by the computerized elastic analysis which were confirmed by the findings of the experimental test results:

1. High stresses that develop at early stages of loading are concentrated around the contact area of the hillside washer with the web.

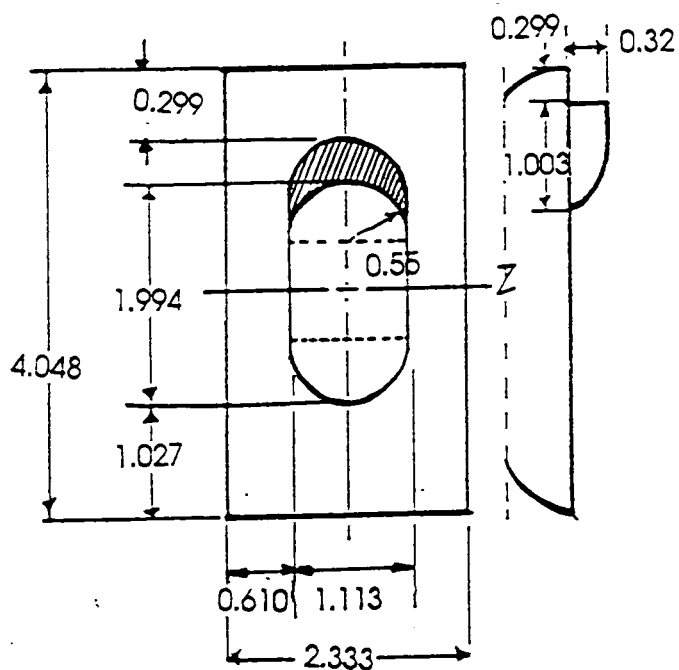
2. Yield stresses in the web plate could be reached around the anchorage point at relatively low levels of pull-out force in comparison with the ultimate load capacity. These high stresses dissipate and decrease in magnitude radially away from the anchorage point to the other weld line between the web plate and the flange of the section. For the size of the test specimen used here, the semi-circular stress distribution fades out to low levels at a radial distance of approximately 8 ins. from the anchorage point.
3. Higher concentrated and localized stresses are also generated on the other side of the web-flange weld line of the section away from the anchorage point.
4. A yield line approach using limit state analysis will be needed to predict the load carrying capacity of the x-brace connection at failure. The yield line analysis is expected to also predict the potential failure mode by virtue of its scanning procedure of the potential failure mechanisms.

ANALYTICAL INVESTIGATION

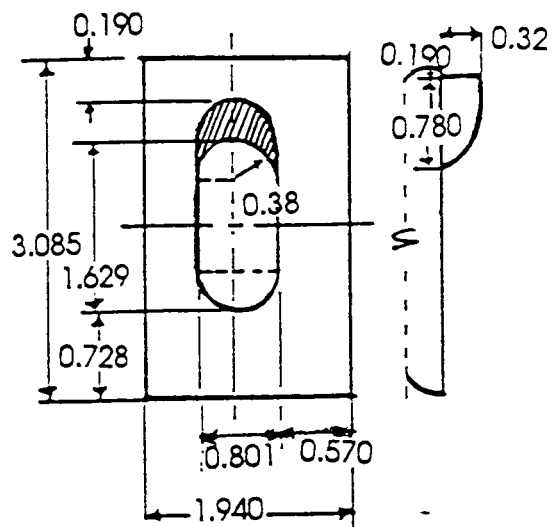
Recent theoretical investigations have been successful in using the yield line approach - failure mechanisms technique - for predicting the ultimate load carrying capacity of steel connections, e.g., Parker and Morris (1977), Parker and Brunno (1986), and Stevens and Kitipornchai (1990). This approach was proposed initially by Johansen (1962) and Hognestad (1953) for

estimating the ultimate capacity of reinforced concrete slabs on the basis of potential failure patterns. The inelastic yield line method finds added support in the arguments used in promoting the strong current trend for the limit state design philosophy of the LRFD specification (AISC 1986). The prediction process on the basis of failure mechanisms or failure patterns for the ultimate load capacity can fairly easily accommodate the stress concentrations, the residual stresses, and the redistribution of stresses. It can allow for a balanced design at failure among the different variables. It is also possible to use an effective failure stress rather than using initial yield or fracture stresses to define failure as suggested by Packer and Bruno (1986) and Stevens and Kitipornchai (1990).

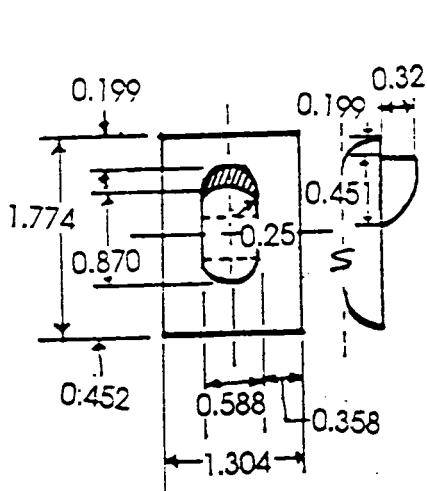
In the following analytical formulations, all prevailing and meaningful failure mechanisms are included in the analysis except for the failure due to the collapse of the hillside washer itself. The washer serves the purpose of transferring the pull-out force from the x-bracing rod to the web plate of the framing section. Its strength is not considered to be a part of the connection and its design is expected to be established by the manufacturer. The contact area between the flat base of the hillside washer and the web of the steel framing is an important parameter in the analysis as it was found to influence the performance of the connection. The geometry of the contact flat base and the nipple engagement of the hillside washers used in the experimental tests of this report are shown in Fig. 6.



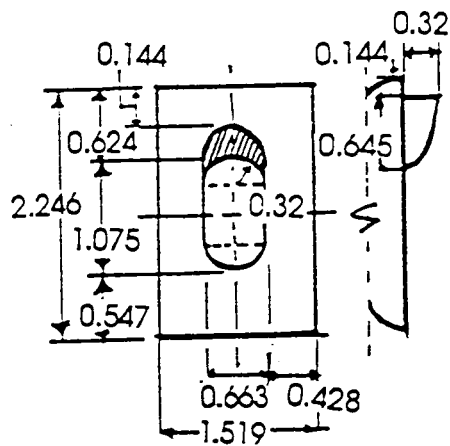
(a) 1" Hillside Washer



(b) 3/4" Hillside Washer



(c) 1/2" Hillside Washer



(d) 5/8" Hillside Washer

FIG. 6. Details of Hillside Washers

FAILURE MECHANISMS AND ANALYTICAL CALCULATIONS

The procedure used in executing the laboratory tests was based on altering the variable parameters one at a time in each of the tests. The observed failure mode was used as a guide in determining the next test set-up. The analytical prediction presented here follows these major parameters of the connection detail and addresses each potential failure mechanism on its own merits.

Failure Mechanism 1: Tensile Failure of the X-Bracing Rod

The ultimate load carrying capacity corresponding to this failure mechanism (P_{u1}) is given by

$$P_{u1} = \frac{\pi d_e^2}{4} (\sigma_{yr})_{eff} \quad (1)$$

in which d_e is the tensile stress diameter at the threaded zone of the rod (AISC 1988), and σ_{yr} is the effective yield stress of the steel rod.

The effective yield stress is assumed to lie somewhere between the ultimate and the actual yield stress. It could be stated that the ultimate strength (σ_u) should be used in this limit state analytical approach, but in general the characteristics of the entire stress versus strain curve have been found to influence the load carrying behavior of steel connections. In contrast to the idealized assumption of uniform plastic stress distribution at failure, the true distribution of the ultimate stress is seldom

uniformly distributed across the section when a plastic hinge failure occurs. The ideally tensile x-bracing rod was forced by the rotation of the hillside washer to bend normal to the deflected shape of the plate of the section. Failure of the bracing rod occurred at that point of contact between the base of the hillside washer and the web plate. The analysis of the actual test results confirmed this observation. The use of an effective yield stress agrees with the findings of Packer and Bruno (1986) and Stevens and Kitipornchai (1990). The suggested effective yield stress $[(\sigma_y)_{eff}]$ used in estimating the plastic capacity of a real section in a connection is given by

$$(\sigma_y)_{eff} = \sigma_y + \frac{2}{3}(\sigma_u - \sigma_y) \quad (2)$$

Note that the difference between the ultimate strength (σ_u) and the effective yield strength $[(\sigma_y)_{eff}]$ as given in Eq. 2 for the x-bracing rods is quite small - see Table 2. The concept of using an effective yield stress is used throughout this report.

The ultimate tensile load of the x-bracing rod as given in Eq. 1 should be the reference, minimum, ultimate capacity that the connection must withstand for a proper connection design.

Failure Mechanism 2 : Weld Failure of the Web-Flange Connection

The weld line between the web and the flange of the section is subjected to a high concentration of localized stresses due to the

pull-out force of the x-bracing rod. Using an effective length of weld and the suggested LRFD (AISC 1986) approach for calculating the ultimate strength capacity of a fillet weld, the strength of the weld adjacent to the anchorage point with only one side of the web plate welded to the flange (Fig. 2) is equal to

$$P_{u2} = 0.6 F_{exx} S_w L_w \left(\frac{D}{D-d} \right) / \sin \theta \quad (3)$$

and for $D = 16.5$ in., $d = 2.5$ ins., and $\theta = 60^\circ$, from the test set-up, then

$$P_{u2} = 0.816 F_{exx} S_w L_w \quad (3a)$$

in which F_{exx} = the classification tensile strength of the weld metal; S_w and L_w = effective throat thickness and the effective length of the adjacent web-flange fillet weld line, respectively - see LRFD (AISC 1986) for the definition of the effective throat thickness, and Fig. 7 for the definition of the effective length of the adjacent fillet weld. The empirical definition of the effective length of weld as shown in Fig. 7 was based on the average of all observations of the yield lines of the initial failure of the test specimens that failed due to weak welds. The leg size of the fillet welds shown in Table 3, Col. 7, were found by physical measurements from each test specimen. Certain variations and inconsistencies in the size, workmanship, and penetration of this weld line over its effective length were clearly evident in most of the test specimens especially when the shielded metal arc process (SMAW) was used for welding. But,

uniform and deeper penetration welds were noted in test specimens when the automatic submerged arc welding method (SAW) was used. Accordingly, the provisions of Section J2.2a of the AISC LRFD Specification (AISC 1986) were found to be applicable. These provisions were used in the calculations for the strength of the weld - Table 4, Col 5.

Failure Mechanism 3: Direct Shear Fracture of the Web Plate -

Direct shear fracture of the web plate at the edge of the weld line, when using the effective weld length L_w , was found to theoretically control the collapse mechanism of the connection for thin and weak base metal webs only. The fillet weld failed before the connecting base metal in all of the test specimen that failed at the web-flange connection because the ultimate shear strength of the base metal was considerably higher than the electrode strength. This observation of the test results confirmed the AISC-LRFD Specifications J4. The mathematical formulation for the direct shear failure, when it controls the failure mechanism, is given by

$$P_{u3} = \frac{1}{\sqrt{3}} \sigma_{yw} t_w L_w \left(\frac{D}{D-d} \right) / \sin \theta \quad (4)$$

and using the data of the test set-up, then Eq. 4 reduces to

$$P_{u3} = 0.785 \sigma_{yw} t_w L_w \quad (4a)$$

in which σ_{yw} = effective yield stress of the web plate as defined by Eq. 2; and t_w = thickness of the web plate.

Failure Mechanism 4: Punching Shear Fracture of the Web Plate

Using a yield line approach for predicting the direct pull-out force required for the hillside washer to punch through the web, then

$$P_{u4} = \tau_{yw} b_o t_w / \sin \theta \quad (5)$$

in which τ_{yw} = effective ultimate punching shear stress of the web plate; b_o = effective perimeter of the flat base of the hillside washer; and t_w = thickness of web plate. The effective shear stress at yield can be related to the effective tensile yield strength of the web plate by any of the familiar failure theories. Using the Tresca yield criteria, then

$$\tau_{yw} = 0.5 \sigma_{yw} \quad (6)$$

or, if the Von Mises failure theory is used, then

$$\tau_{yw} = 0.577 \sigma_{yw} \quad (7)$$

But, using the AISC LRFD Specifications approach for the shear strength on an effective area, yields

$$\tau_{yw} = 0.60 F_{yw} \quad (8)$$

The difference between these three shear stress correlations, Eqs. 6, 7, and 8, is academic and relatively small. For this reason, Eq. 7 is used in the calculations of the effective ultimate punching shear strength at failure.

The effective punching shear perimeter of the contact area of the hillside washer with the web, b_o , was found to be related to the size of the slotted hole in the web through which the x-bracing rod passes. The net effective perimeter was assumed on the basis of the test results to be equal to the actual perimeter of the base of the hillside washer reduced by the size of the slotted hole in the web. The net effective perimeter is then equal to

$$b_o = 2[(B+b) - (L+h)] \quad (9)$$

in which B and b = length and width of the contact area of the base of the hillside washer respectively; and L and h = length and width of the slotted hole in the web plate.

Using Eqs. 7 and 9, the ultimate load carrying capacity for this failure mechanism, Eq. 5, can be written as

$$P_{u4} = 1.154 [(B+b) - (L+h)] \sigma_{yw} t_w / \sin \theta \quad (5a)$$

Failure Mechanism 5: Tensile Fracture of the Web Plate

The details of the protruding rounded nipples of the hillside washers that fit into the slotted hole of the web plate are shown in Fig. 6. The in-plane parallel to the web component of the pull-out force was found to induce direct tensile stresses that eventually caused a tensile mode fracture of the longitudinal sides of the slotted hole as shown in Fig. 8. This localized fracture caused the hillside washer to rip through the slotted hole under the effect of the pull-out force.

A direct yield line approach for the prediction of the ultimate load was also possible for this mode of failure on the basis of the observations made during the execution of the actual tests and the test results. The observed failure confirmed the finite element elastic analysis predictions of complete yielding of the area under the hillside washer. Plastic flow of the web plate around the hillside washer was clearly evident in the tests. Tensile fracture occurred along the two longitudinal sides of the slotted hole as the pull-out force exhausted the plasticity of the web metal. The ultimate pull-out load was formulated on the basis of the combined effects of the direct bearing and tensile stresses under the hillside washer as follows

$$P_{u5} = 1.154 \sigma_{yw} / [\cos \theta / (b-h)t_w + \sin \theta / (Bb-Lh)] \quad (6)$$

in which $(b-h)$ = net width of the web plate bounded by sides of the hillside washer and $(Bb-Lh)$ = net bearing area under the base of the hillside washer - see Fig. 4.

COMPARISON OF EXPERIMENTAL VERSUS ANALYTICAL RESULTS

The preceding analytical approach was based on using yield line, limit state, approach for each of the independent failure mechanisms. The predicted analytical values for the ultimate loads were verified by the results of the laboratory experimental testing program. The independent variables were altered individually in each test set-up in order to demonstrate the impact of each variable on the ultimate load and the failure mechanism. The failure mode predicted by the analytical approach was checked against that observed in the actual test.

The predicted failure loads, $P_{u1} - P_{u5}$, from each of the five failure mechanisms are shown in Table 4, Cols. 4-8. The lowest predicted value, the controlling value, is underlined in the listing. The experimental ultimate loads, P_{uexp} , are also shown in Table 3, Col. 3. The ratios of P_{uexp}/P_u are listed in Col. 9. The failure mode from the test and that corresponding to lowest analytical P_u value are shown in Cols. 10 and 11, respectively. It can be seen that the agreement between the analytical predictions and the test results for both the ultimate load capacities and the failure modes is generally very good. The noticeable exception is with the cases of weld failures. This was attributed to the inconsistency in the workmanship and quality of the weld as noted earlier.

In the GS-Series, the weld lines between the web and the flanges were placed using the automatic submerged arc welding method (SAW). This welding option provided, as expected, superior quality and deeper penetration welds. The stronger weld lines in this series of tests prevented premature weld failure. The patch stiffener that was used to strengthen the web plate prevented the local failure of the connection. Tensile rod failure was predicted for all of the tests in this series. The test results confirmed the predictions of the analytical analysis.

In the BS-Series of the test specimens, welding was excessively done as to the thickness and number of passes as indicated in Table 3. The intentional over-welding in this series of tests influenced, as expected, the failure mode of the tested specimens.

The comparative analysis of the theoretical values versus the test results emphasize the significance of the two main variables: (1) the size of the x-bracing rod and (2) the strength of the web-flange weld. The static test results indicated that if these two variables are designed to sustain a given load, then the failure criteria rests on the geometry of the flat contact area between the hillside washer and the slotted web of the section. The test and theoretical results have indicated that, with an adequate web-flange weld, it is possible to design an anchorage connection capable of withstanding the full tensile strength of the x-bracing rod or the maximum load that the framing section can withstand, whichever is smaller. From a seismic loading point of view, this is important because of the potential use of the anchorage connection as a damping mechanism to control the response of the framing structure during extreme seismic activities.

REPETITIVE TENSILE LOADING TESTS - SEISMIC LOADING

A pre-established maximum pull-out force was applied for 20 cycles in this series of tests. The load was set on the basis of the results from the static loading of similar test specimens. If failure did not occur during this repetitive cyclic loading, then the pull-out direct tensile load was increased until failure occurred. The load-deflection of the web plate at the point of loading was recorded for comparative analysis between the different tests. The tension only hysteresis loop was used to detect deterioration in the stiffness of the connection under cyclic loading. The basic parameters of the test specimens are shown in

Table 5. The test results and the predicted ultimate load capacities with the failure modes are shown in Table 6. The recorded load-deflection diagrams are shown in Figs. 9-15.

Loading up to the yield point of the x-bracing rod was used in the test set-ups where the rod tensile failure was expected to control the ultimate load. In the remainder of the test set-ups, the predetermined upper limit on the repetitive cyclic load was set so that yielding will occur somewhere at that load in the anchorage connection. The lower limit on the tensile repetitive cyclic load was 500 pounds.

The influence of the size of the hillside washer on the failure load was investigated by over-sizing the washer while keeping all other variables the same. In Test No. 2, the size of the hillside washer was larger than that of the rod, 3/4 versus 5/8 in. While in Test No. 1, 5/8 in. for both the rod and the washer were used. The tensile strength of the rod controlled the failure mode in Test No. 2, and the tensile fracture strength of the web plate controlled the ultimate load in Test No 1.

Failure of the weld between the web and the flange adjacent to the pull-out force was not a serious failure mechanisms in the repetitive loading tests because the weld was oversized, carefully placed, and with full penetration in almost all of the test specimens. Accordingly, premature weld failure did not occur and the predetermined maximum repetitive cyclic load was sustained by all of the test set-ups.

The 20 cycles of repetitive loading were applied continuously at an approximate rate of six seconds per cycle. The load-

Table 5. Test Specimens Parameters - Repetitive Tests

Test No.	Test Specimen	PROPERTIES					
		Web (t_w) (in.)	Web Stiffener	Rod (d) (in.)	Washer Size (in.)	Web-Flange Weld	
						Leg Size (in.)	Rating
(1)	(2)	(3)	(4)	(5)	(6)	(7)	(8)
1	RCC 1/8 R 5/8A	0.127	————	5/8	5/8	0.16	Two passes
2	RCC 1/8 R 5/8B	0.127	————	5/8	3/4	0.12	Good
3	RCC 1/8 R 3/4A	0.128	————	3/4	3/4	0.12	Good
4	RCC 1/8 R 3/4B	0.126	————	3/4	3/4	0.12	Good
5	RCC 1/4 R 1	0.249	————	1	1	0.21	Two passes
6	RGP 3/16 R 3/4A	0.178	Patch Plate	3/4	3/4	0.20	Excellent
7	RGP 3/16 R 3/4B	0.178	Patch Plate	3/4	3/4	0.20	Excellent
8	RBS 1/8 R 3/4	0.118	Trans. Stiffeners	3/4	3/4	0.18	Good
9	RBS 3/16 R 3/4	0.177	Trans. Stiffeners	3/4	3/4	0.19	Good
10	RBS 1/4 R 1	0.249	Trans. Stiffeners	1	1	0.22	Two passes

Table 6. Comparison of Experimental and Analytical Results - Repetitive Tests

Test No.	Test Specimen	Repetitive Load		Ultimate Loads (lbs.)						Ratio: $\frac{P_{uexp}}{P_u}$	Failure Mode	
				Experiment P_{uexp}	Analytical as per Failure Modes						Test	Theory
		Prep (lbs.)	No. of Cycles		P_{u1}	P_{u2}	P_{u3}	P_{u4}	P_{u5}			
(1)	(2)	(3)	(4)	(5)	(6)	(7)	(8)	(9)	(10)	(11)	(12)	(13)
1	RCC 1/8 R 5/8A	14,000	15	14,000	16,374	23,515	31,276	12,692	12,914	1.08	5	5
2	RCC 1/8 R 5/8B	15,000	10	15,000	16,374	20,146	36,006	28,672	21,885	0.92	1	1
3	RCC 1/8 R 3/4A	15,000	20	19,900	27,278	20,146	36,006	28,672	22,048	0.99	2	2
4	RCC 1/8 R 3/4B	15,000	20	18,000	27,278	20,146	35,443	28,224	21,721	0.90	2	2
5	RCC 1/4 R1	30,000	20	38,250	48,478	40,561	80,586	82,890	57,792	0.94	2	2
6	RGP 3/16 R 3/4A	18,000	20	*	27,278	47,491	53,253	88,622	60,806	—	—	—
7	RGP 3/16 R 3/4B	22,000	20	*	27,278	47,491	53,253	88,622	60,806	—	—	—
8	RBS 1/8 R 3/4	15,000	20	17,500	27,278	30,218	33,857	23,997	18,406	0.95	5	5
9	RBS 3/16 R 3/4	21,500	20	27,000	27,278	31,897	50,785	35,996	26,988	1.00	1	1 or 5
10	RBS 1/4 R1	30,000	20	42,500	48,478	42,495	82,198	84,548	53,595	1.00	2	2

* Test terminated before connection failure is reached because of excessive deflection of web and deformation of entire test section.

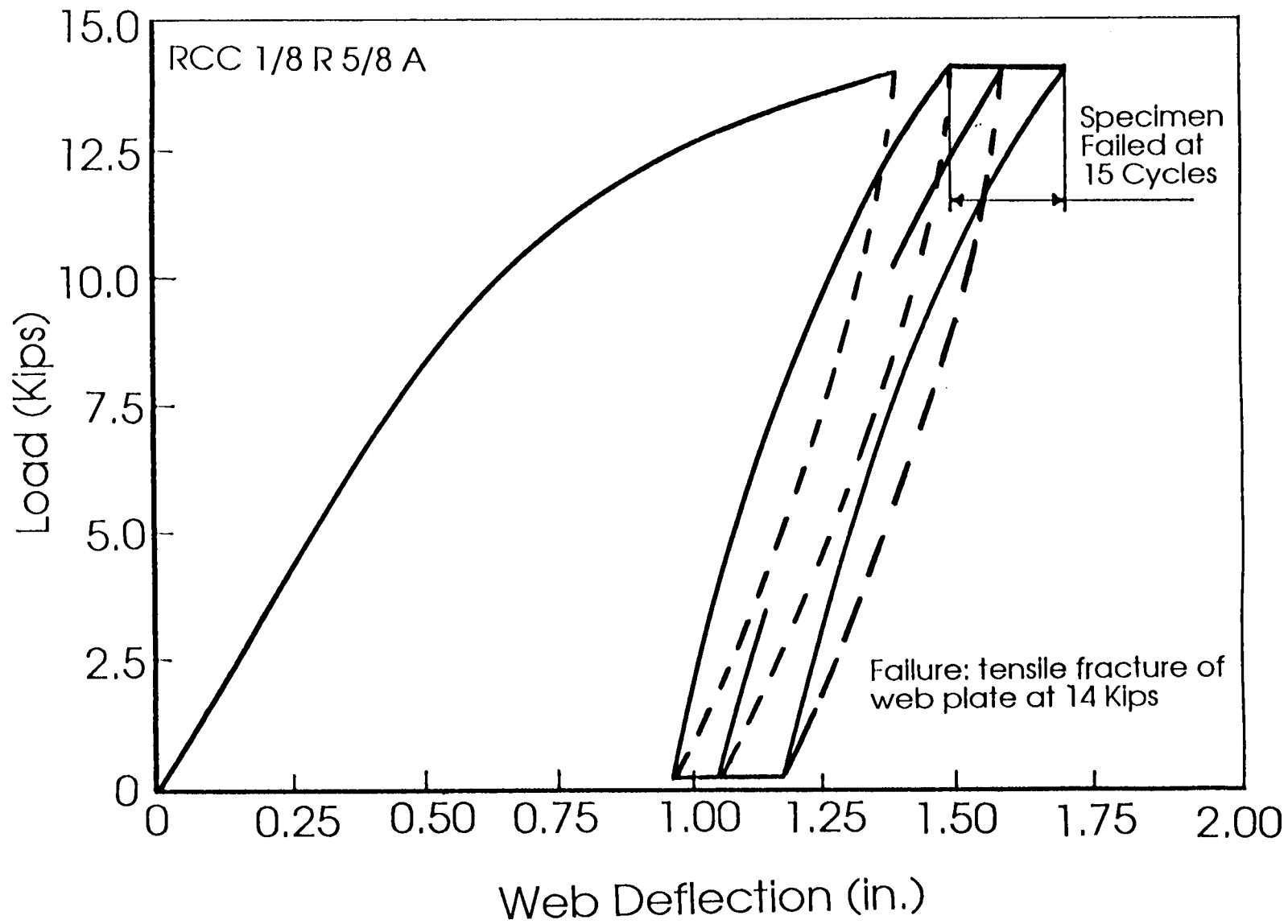


FIG. 9. Load versus Web Deflection for repetitive Tensile Loading (RCC 1/8 R 5/8)

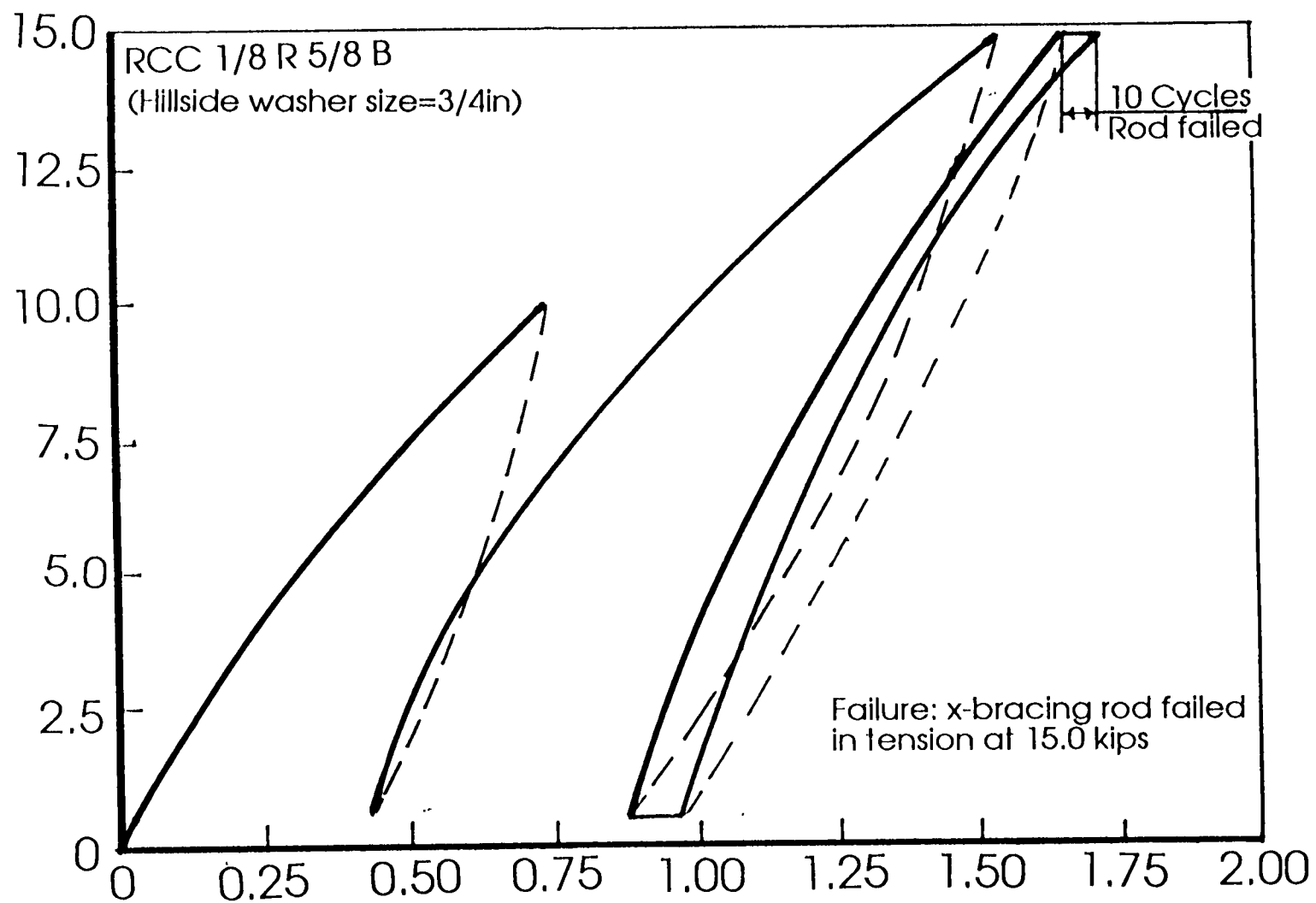


FIG. 10. Load versus Web Deflection for repetitive Tensile Loading (RCC 1/8 R 5/8 B)

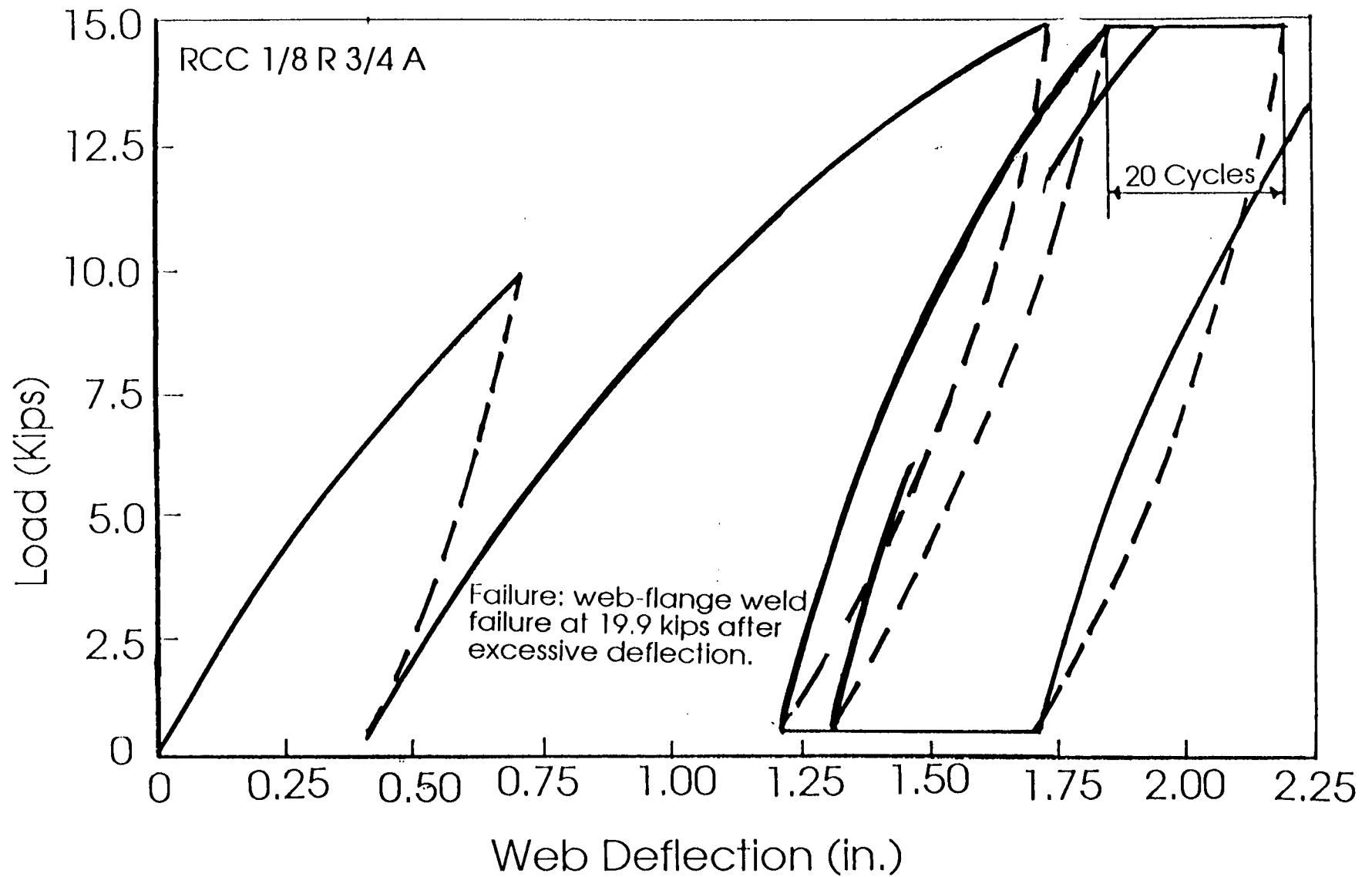


FIG. 11. Load versus Web Deflection for repetitive Tensile Loading (RBS 1/8 R 3/4 B)

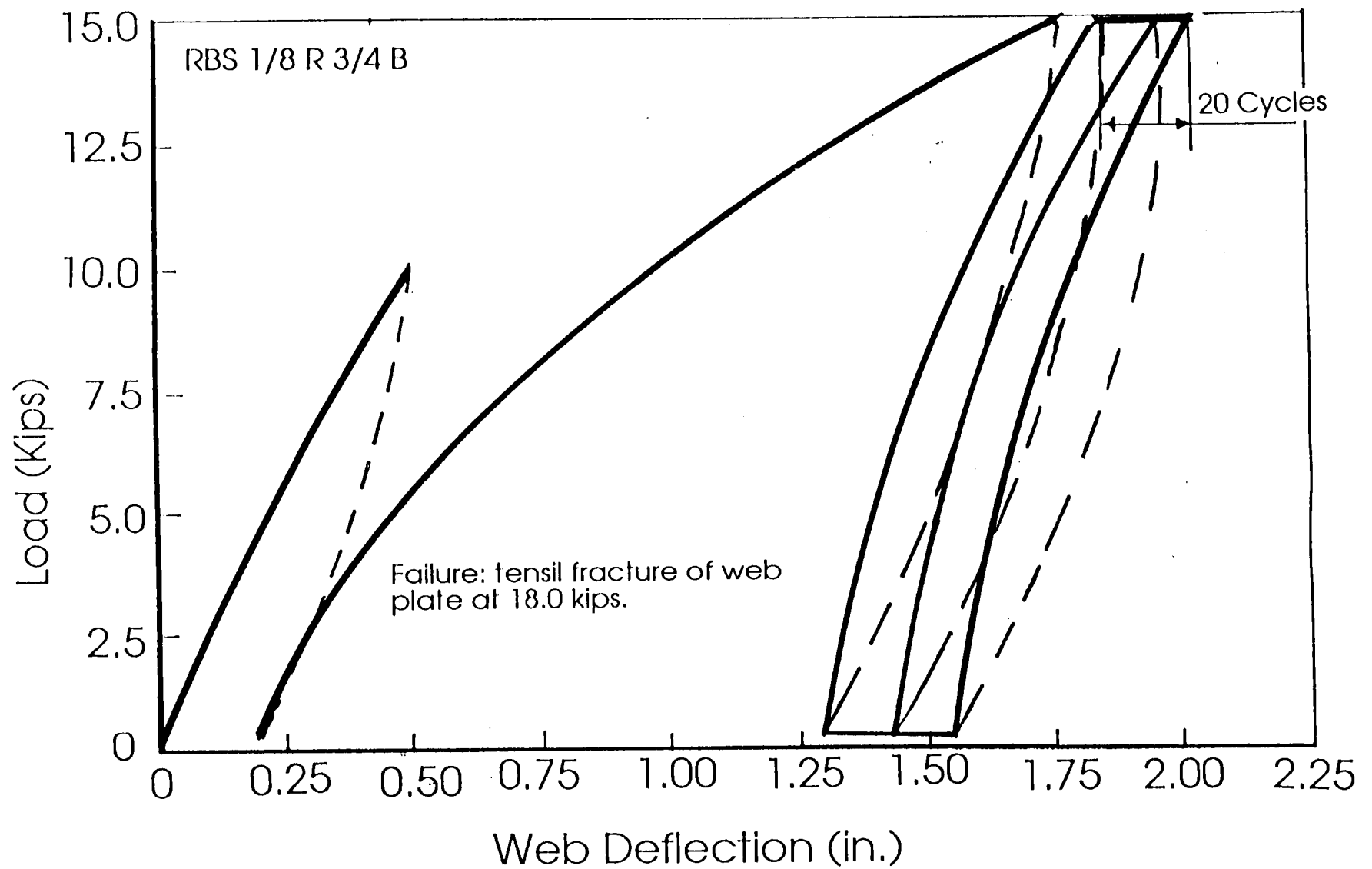


FIG. 12. Load versus Web Deflection for repetitive Tensile Loading (RCC 1/8 R 5/8 B)

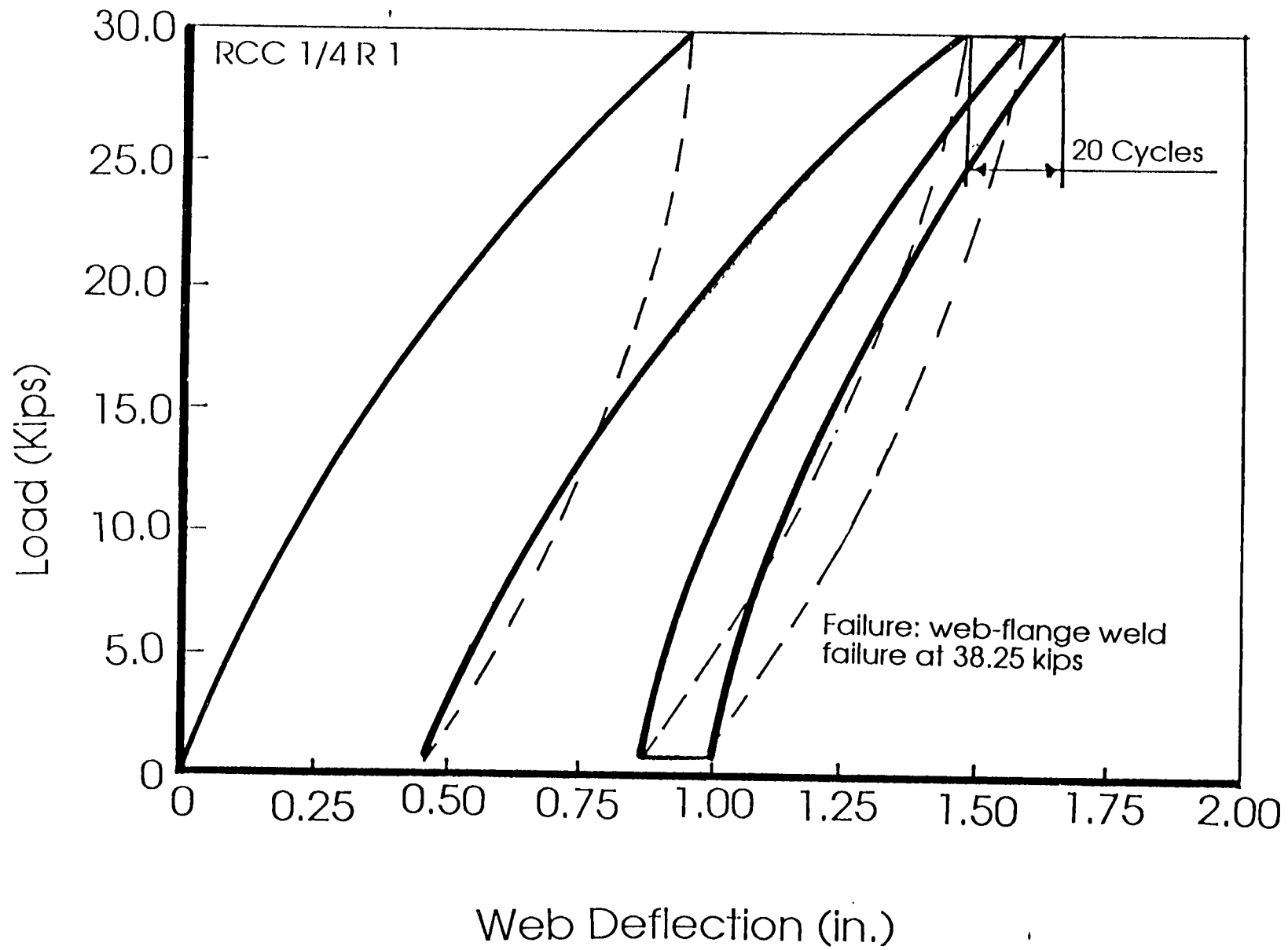


FIG. 13. Load versus Web Deflection for repetitive Tensile Loading (RCC 1/4 R 1)

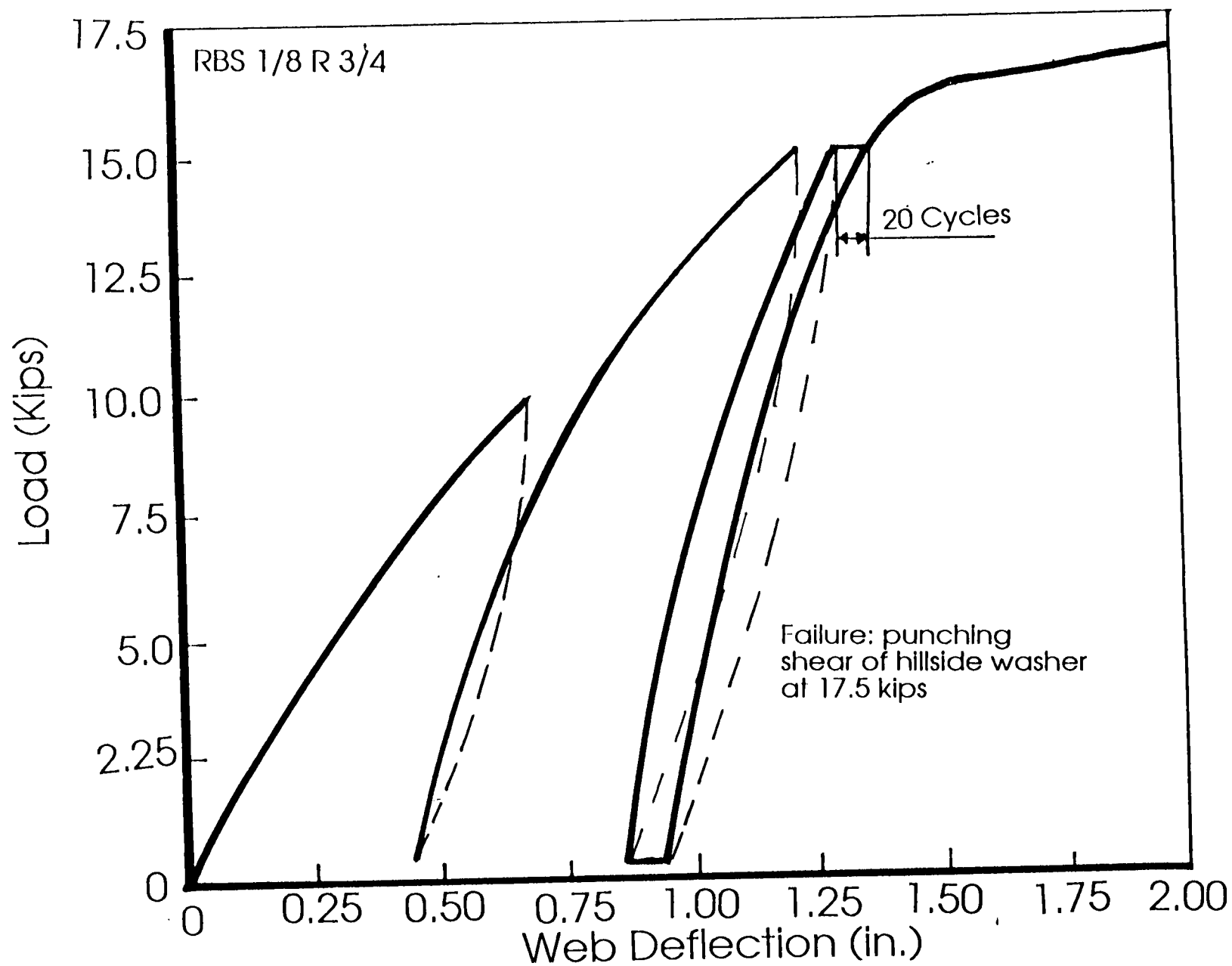


FIG. 14. Load versus Web Deflection for repetitive Tensile Loading (RBS 1/8 R 3/4)

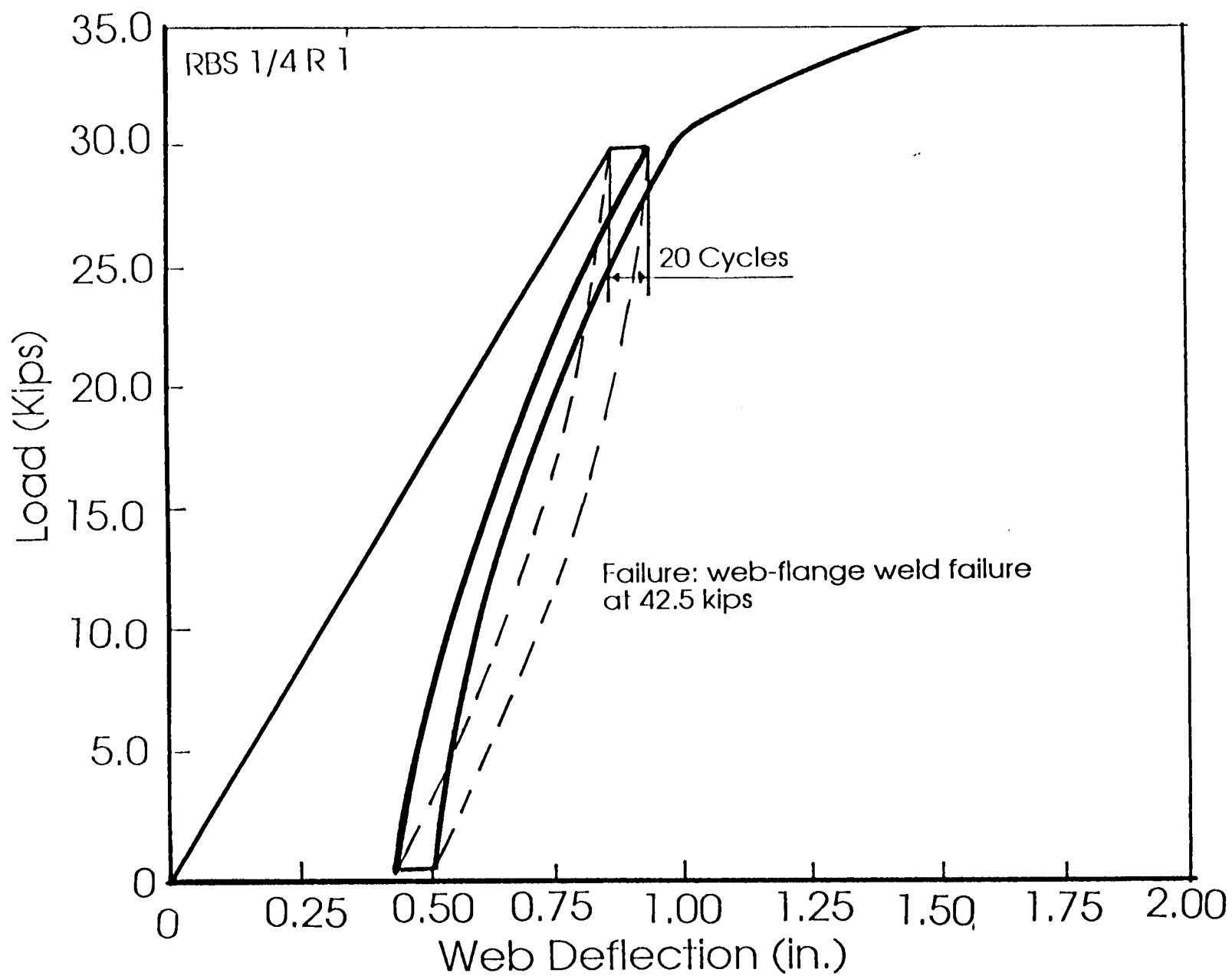


FIG. 15. Load versus Web Deflection for repetitive Tensile Loading (RBS 1/4 R 1)

deformation curves have clearly indicated among other things that when the loading of the specimen was carried far enough to produce plastic strains in the connection, then the unloading-loading in the follow-up cycles did not influence the ultimate load carrying capacity of the connection. The plastic strains established in the first and second cycles of loading did not increase significantly in the follow-up cycles. This observation demonstrated a significant and a highly desirable damping characteristic associated with the anchorage connection in view of the excessive deformation exhibited by the web plate of the section - see Figs. 9-15. The overall evaluation of the test results showed that there was no deterioration in the strength of the connection at the end of the 20 cycles of repetitive loading.

The loading was extended beyond the 20 repetitive cycles by monotonically increasing the direct pull-out force to failure. The test results indicated that the connection sustained the loading up to the expected ultimate strength but at a relatively lower ductility than that of the static loading. Thus, the combined effect of any work-hardening process and strength reduction factors, such as Bauschinger effect and the residual deformation left from the plastic hinge formation during the initial loading, resulted in maintaining the static ultimate load capacity. On the other hand, it should be noted that deterioration in the strength of such connections under seismic loading has been erroneously assumed and taken for granted by many designers. The deterioration in steel connections is usually associated with the compression leg of the hysteresis loop and does not necessarily apply to the

tensile x-bracing. The test results confirmed that deterioration did not occur in the connection. It is felt that more controlled seismic load simulation tests on a framed structure will be needed in order to elaborate quantitatively on this observation.

CONCLUSIONS

The experimental testing program coupled with the analytical formulations presented here have permitted the evaluation of the various parameters that could lead to the collapse of the currently used anchorage connection for x-bracing rods or cables in low rise metal buildings. A hillside washer bearing on the flat web of the framing section is assumed to be used in the anchorage detail.

The following conclusions can be made on the basis of the test results for static and repetitive loading conditions.

1. The geometry and size of the net contact area between the flat base of the hillside washer and the web of the structural section is of primary importance in the design of the connection.
2. Premature failure could occur in the web-flange weld next to the x-bracing anchorage connection if the size of the structural framing weld of the section is not checked for the effects of the load carried by the x-bracing rod. The effective length of the web-flange weld line that contributes to the resistance of the concentrated x-bracing force is concentrated around the length of the longitudinal side of the hillside washer. With proper weld size, penetration and quality, a premature failure of the web-flange weld connection

can be avoided.

3. Additional welding along the effective length of the weld over and above that required for the structural framing of the section will generally be needed for the full development of the anchorage connection.
4. Localized yielding of the web plate due to stress concentration around the anchorage connection usually develop at the early stages of loading. Neither the transverse stiffener nor the patch plate stiffener to the web plate will restrain or eliminate the yielding from taking place. However, using a patch plate to stiffen the web plate could provide the local strengthening required to prevent the hillside washer from punching through the web plate.
5. Plastic deformation of the anchorage connection can be excessive before failure takes place if premature failure of the web-flange weld is prevented. The plastic deformation of the web plate and the anchorage connection detail as a whole could be used to dampen the seismic response of the framed metal building.
6. Repetitive tensile loading beyond yielding of the anchorage connection did not cause serious deterioration to the ultimate strength of the connection after 20 cycles of loading.
7. The load carrying capacity of the anchorage connection can be predicted fairly successfully using limit state design approach. The predicted ultimate loads and failure modes were in good agreement with the test results.

APPENDIX I. REFERENCES

- Bridgman, P.W. (1952). *Studies in large plastic flow and fracture*. McGraw-Hill Book Company, New York, N.Y.
- Chang, K.C., Hwang, J.S., and Lee, G.C. (1989). "Shaking table study of a 1/5 scale steel frame composed of tapered members." *Tech. Report NCEER-89-0024*, State Univ. of N.Y., Buffalo, N.Y.
- Hognestad, E. (1953). "Yield-Line Theory for the Ultimate Flexural Strength of Reinforced Concrete Slabs." *J. ACI*, 24, No. 7, *Proc.*, 49, p. 637.
- Hwang, J.S., et. al. (1989). "Shaking table tests of pinned-base steel gable frames." *J. Struct. Engrg.* 115 (12), 3031-3043.
- Johansen, K.W. (1962). *Yield line theory*. English translation, Cement and Concrete Assoc., London, U.K.
- Kitipornchai, S., and Traves, W.H. (1989). "Welded tee end connections for circular hollow tubes." *J. Struct. Engrg.*, ASCE, 115 (12), 3155-3170.
- "Load and resistance factor design specifications for structural steel buildings. (1986). American Institute of Steel Construction, Chicago, Ill.
- "Loma Prieta (San Francisco) earthquake of October 17, 1989 - Building Survey of the Epicenter area." (1980). Metal Building Manufacturers Association, Cleveland, Ohio.
- "Low rise systems manual." (1986). Metal Building Manufacturers Association, Cleveland, Ohio.
- Packer, J.A. and Morris, G.A. (1977). "A limit state design method for the tension region of bolted beam-column connections." *The Struct. Engrg.*, 55(10), 446-458.
- Packer, J.A. and Brunno, L. (1986). "Behavior of bolted flange-plate connections in rectangular hollow section tension members." *Proc. 10th Australasian Conf. on Mechanics of Structures and Materials*, Adelaide, Australia, 45-50.
- Popov, E.P., and Black, R.G. (1981). "Steel struts under severe cyclic loadings." *J. Struct. Div.*, ASCE, 107(9), 1857-1881.
- SEAOC Seismology Committee. (1990). "Recommended lateral force requirements and commentary." Structural Engineers Association of California, Sacramento, California.
- Stevens, N.J. and Kitipornchai, S. (1990). "Limit analysis of welded tee and end connections for hollow tubes." *J. Struct. Engrg.*, ASCE, 116(9), 2309-2322.

APPENDIX II. NOTATION

The following symbols are used in this paper:

- B = length of flat base of hillside washer;
- b = width of flat base of hillside washer;
- D = depth of framing section;
- d = distance from the anchorage point to the adjacent flange;
- d_e = effective diameter of x-bracing rod at the root of the threaded section;
- F_{exx} = classification strength of the weld metal;
- h = width of slotted hole in web plate at connection;
- L = length of slotted hole in web plate at connection;
- L_w = effective length of web-flange weld;
- P_{rep} = maximum repetitive load applied in the cyclic loading tests;
- $P_u, P_{u1} - P_{u5}$ = analytical ultimate load capacity of connection, and corresponding values for modes 1 to 5;
- P_{uexp} = experimental ultimate load capacity of connection;
- S^w = effective throat thickness of web-flange fillet weld, see LRFD (AISC 1986);
- t_w = thickness of web plate of framing section;
- T_{yw} = effective yield punching shear strength of web plate;
- θ = the vertical angle of x-bracing rod with the web;
- σ_y, σ_u = yield and ultimate tensile strength, respectively; and
- σ_{yr}, σ_{yw} = yield strength of x-bracing rod and web plate, respectively.

APPENDIX III. DESIGN OF ANCHORAGE CONNECTION USING ALLOWABLE STRESS DESIGN (ASD)

The prediction process and formulations presented in this report are based on limit state design-ultimate strength. The equations are directly applicable and can be used with the AISC load and resistance factor design method (LRFD) after incorporating the appropriate resistance factor (ϕ) into the nominal strength equations of P_u . The design strength is then calculated for each applicable limit state, failure mechanism, as $(\phi) P_u$ (AISC 1986).

In order to convert the prediction equations presented in this report to a working stress design formulations, it is recommended to incorporate an appropriate safety factor for each of the failure mechanisms as follows:

Failure Mechanism 1: Tensile Failure of X-Bracing Rod - Eq. 1

Using 1/3 of the effective yield strength of the rod for the allowable tensile stress on the net area at the threads, then Eq. 1 can be written as

$$P_1 = 0.26 \sigma_{yr} d_e^2 \quad (1-ASD)$$

in which σ_{yr} is the effective yield tensile strength of the x-bracing rod - see Eq. 2.

Failure Mechanism 2: Weld Failure of the Web-Flange Connection - Eq. 3

The allowable shear load for a fillet weld is recommended to be taken as 0.3 of the classification nominal tensile strength of

the weld, and Eq. 3 can be written as

$$P_2 = 0.30 F_{exx} S_w L_w \left(\frac{D}{D-d} \right) / \sin \theta \quad (2-ASD)$$

For a weld size equal to or less than 1/8 in., a higher factor of safety might be justified to be used in the above equation.

Failure Mechanism 3: Direct Shear Fracture of the Web Plate - Eq. 4

The allowable load for this failure mechanism is recommended to be based on 0.3 of the effective yield tensile strength of the web metal, and Eq. 4 can be written as

$$P_3 = 0.3 \sigma_{yw} t_w L_w \left(\frac{D}{D-d} \right) / \sin \theta \quad (3-ASD)$$

Failure Mechanism 4: Punching Shear Fracture of the Web Plate - Eq. 5

Using 0.3 of the effective yield tensile strength of the web metal for the allowable punching shear stress, then Eq. 5 can be written as

$$P_4 = 0.6[(B+b)-(L+h)] \sigma_{yw} t_w / \sin \theta \quad (4-ASD)$$

Failure Mechanism 5: Tensile Fracture of the Web Plate-Eq. 10

The allowable tensile load for the web metal is recommended to be taken as 1/2 its effective yield tensile stress, and Eq. 10 can be written as

$$P_5 = 0.577 \sigma_{yw} / [\cos \theta / (b-h) t_w + \sin \theta / (Bb-Lh)] \quad (5-ASD)$$

APPENDIX IV. NUMERICAL EXAMPLE

Rod; diameter = 3/4 in., $d_e = 0.68$ in., $\sigma_{yr} = 75.15$ ksi

Hillside washer; Bxb = 3.085x1.940 in.

Fillet weld; $F_{exx} = 60$ ksi, Leg size = 0.11 in.

Web plate; $t_w = 0.186$ in, $\sigma_{yw} = 73.9$ ksi, D = 16.5 in., d = 2.5 in.

Slotted hole; L = 1.875 in., h = 0.875 in., $\theta = 60^\circ$

Theoretical Ultimate Strength: (See Table 4, Test No. 10)

1. $P_{u1} = \frac{\pi \times (0.68)^2 \times 75.15}{4} = \underline{27.28 \text{ kips}}$
2. P_{u2} ; $L_w = \frac{B+2(d-b)}{2} \tan(30^\circ) = \frac{3.085+2(2.5-1.94)}{2} (.578) = 4.85 \text{ in.}$
 $P_{u2} = 0.6 \times 60 \times 0.707 \times 0.11 \times 4.85 \times \frac{16.5}{16.5-2.5} \times \frac{1}{0.866} = \underline{18.47 \text{ kips}}$
3. $P_{u3} = 0.577 \times 73.9 \times 0.186 \times 4.85 \times \frac{16.5}{16.5-2.5} \times \frac{1}{0.866} = \underline{52.33 \text{ kips}}$
4. $P_{u4} = 1.154 [(3.085+1.940) - (1.875+0.875)] \times 73.9 \times 0.186 \times \frac{1}{0.866}$
 $= \underline{41.67 \text{ kips}}$
5. $P_{u5} = 1.154 \times 73.9 / [0.5 / (1.94 - 0.875) 0.186 + 0.866 / (3.085 \times 1.94 - 1.875 \times 0.875)] = \underline{31.31 \text{ kips}}$

Failure Mechanisms 2 controls, weld failure, $P_u = \underline{18.47 \text{ kips}}$

Allowable Stress Design (Eq. 1-5 ASD):

1. $P_1 = 9.03 \text{ kips}$ - Allowable tensile force on x-bracing rod.
2. $P_2 = 9.23 \text{ kips}$ - Allowable force by web-flange weld.
3. $P_3 = 27.20 \text{ kips}$ - Allowable force by direct shear of web plate.
4. $P_4 = 21.66 \text{ kips}$ - Allowable force by punching shear of hillside washer.

5. $P_5 = 15.65$ kips - Allowable force by tensile fracture of web plate.

Design is controlled by the allowable force in the x-bracing rod.

APPENDIX IV. CONVERSION TO SI UNITS

<u>To Convert</u>	<u>To</u>	<u>Multiply By</u>
lbm	kg	0.4536
lbf	N	4.448
ft	m	0.3048
kips	kN	4.448
ksi	kPa	6,895